3-D Adaptive Wind Field Simulation Including Effects of Chimney Emissions

Article · January 2004

CITATIONS
5

READS
83

5 authors, including:

Rafael Montenegro
Universidad de Las Palmas de Gran Canaria
132 PUBLICATIONS **1,208** CITATIONS
SEE PROFILE

Gustavo Montero
Universidad de Las Palmas de Gran Canaria
121 PUBLICATIONS **1,028** CITATIONS
SEE PROFILE

J. M. Escobar
Universidad de Las Palmas de Gran Canaria
93 PUBLICATIONS **986** CITATIONS
SEE PROFILE

Eduardo Rodríguez
Universidad de Las Palmas de Gran Canaria
85 PUBLICATIONS **848** CITATIONS
SEE PROFILE

COMPUTATIONAL MECHANICS
WCCM VI in conjunction with APCOM'04, *Sept. 5-10, 2004, Beijing, China*

3-D Adaptive Wind Field Simulation Including Effects of Chimney Emissions

R. Montenegro*, G. Montero, J.M. Escobar, E. Rodríguez, J.M. González-Yuste

University Institute of Intelligent Systems and Numerical Applications in Engineering, University of Las Palmas de Gran Canaria, Edif. Central Parque Científico-Tecnológico, Campus Universitario de Tafira, 35017 Las Palmas de Gran Canaria, Spain
e-mail: rafa@dma.ulpgc.es, gustavo@dma.ulpgc.es, jescobar@dsc.ulpgc.es, barrera@dma.ulpgc.es, josem@sinf.ulpgc.es

Abstract Air pollution models usually start from the computation of the velocity field of the fluid. In this paper, we present a model for computing such a field based on the contribution of the observed wind flow and the vertical buoyancy or momentum plume rise defined by a Gaussian plume model. This initial velocity field is adjusted to verify incompressibility and impermeability conditions by using a mass consistent model. In this environmental modelling that occur in a three-dimensional domain defined over complex terrain, a mesh generator capable of adapting itself to the topographical data and to the numerical solution is essential. Here, the unstructured tetrahedral meshes are generated by combining the use of a refinement/derefinement algorithm for two-dimensional domains and a tetrahedral mesh generator based on Delaunay triangulation. Occasionally in this process, low quality or even inverted elements may appear. For this reason, we have developed a simultaneous untangling and smoothing procedure to optimise the resulting meshes. Once we have constructed the adapted mesh in accordance with the geometrical characteristics of our domain, we use an adaptive local refinement in the plume trajectory and also for improving the numerical solution. Finally, this model is applied in a test problem.

Key words: 3-D wind modelling and simulation, mass consistent models, Gaussian pollutant plumes, finite element method, mesh refinement.

AUTOMATIC MESH GENERATION ADAPTED TO A SURFACE

In [1, 2] the authors propose a mesh generator for environmental problems which is applied in this model and summarised in this section. The studied domain is limited in its lower part by the terrain and in its upper part by a horizontal plane placed at a height at which the magnitudes under study may be considered steady. The lateral walls are formed by four vertical planes. The generated mesh could be used for numerical simulation of natural processes which have the main effect on the proximities of the terrain surface. Thus node density increases in these areas accordingly. To construct the Delaunay triangulation [3] we must define a set of points within the domain and on its boundary. These nodes will be precisely the vertices of the tetrahedra that comprise the mesh. Point generation on our domain will be done over several layers, real or fictitious, defined from the terrain up to the upper boundary. Specifically, we propose the construction of a regular triangulation of this upper boundary. Now, the refinement/derefinement algorithm [4, 5] is applied over this regular mesh to define an adaptive node distribution of the layer corresponding to the terrain surface and the functions which represent the chimneys. Once the node distribution is defined on the terrain and the upper boundary, we begin to distribute the nodes located between both layers. A vertical

spacing function is involved in this process. This node distribution will be the input to a three-dimensional mesh generator based on Delaunay triangulation [6]. To avoid conforming problems between mesh and orography, the tetrahedral mesh will be designed with the aid of an auxiliary parallelepiped. We start defining the set of points in the real domain and transforming them to this auxiliary parallelepiped where the mesh is constructed. Next, the points are placed by the appropriate inverse transformation in their real location, keeping the mesh topology.
In finite element simulation the mesh quality is a crucial aspect for good numerical behaviour of the method. In a first stage, our automatic 3-D mesh generator constructs meshes with poor quality and, in special cases, for example when node movement is required, inverted elements may appear. So, it is necessary to develop a procedure that optimises the pre-existing mesh. This process must be able to smooth and untangle the mesh. The most usual techniques to improve the quality of a *valid* mesh are based upon local smoothing. In short, these techniques consist of finding the new positions that the mesh nodes must hold, in such a way that they optimise an objective function. Such a function is based on a certain measurement of the quality of the *local submesh*, $N(v)$, formed by the set of tetrahedra connected to the *free node* v. As it is a local optimisation process, we can not guarantee that the final mesh is globally optimum. Nevertheless, after repeating this process several times for all the nodes of the current mesh, quite satisfactory results can be achieved. Usually, objective functions are appropriate to improve the quality of a valid mesh, but they do not work properly when there are inverted elements. This is because they present singularities (barriers) when any tetrahedron of $N(v)$ changes the sign of its Jacobian determinant. In [7] we propose a procedure for untangling and smoothing in the same stage. For this purpose, we use a suitable modification of the objective function such that it is regular all over $\mathbb{R}^3$. When a feasible region (subset of $\mathbb{R}^3$ where v could be placed, being $N(v)$ a valid submesh) exists, the minima of the original and modified objective functions are very close and, when this region does not exist, the minimum of the modified objective function is located in such a way that it tends to untangle $N(v)$. The latter occurs, for example, when the fixed boundary of $N(v)$ is tangled. With this approach, we can use any standard and efficient unconstrained optimisation method to find the minimum of the modified objective function, see for example [8]. We have applied the proposed modification to one objective function derived from an *algebraic mesh quality metric* studied in [9].

LOCAL MESH REFINEMENT

We propose a local refinement algorithm [10] based on the 8-subtetrahedron subdivision developed in [11]. Consider an initial triangulation τ_1 of the domain given by a set of n_1 tetrahedra $t_1^1, t_2^1, ..., t_{n_1}^1$. Our goal is to build a sequence of m levels of nested meshes $T = \{\tau_1 < \tau_2 < ... < \tau_m\}$, such that the level τ_{j+1} is obtained from a local refinement of the previous level τ_j. The error indicator ϵ_i^j will be associated to the element $t_i^j \in \tau_j$. Once the error indicator ϵ_i^j is computed, such element must be refined if $\epsilon_i^j \geq \theta \epsilon_{\max}^j$, being $\theta \in [0,1]$ the refinement parameter and $\epsilon_{\max}^j$ the maximum value of the error indicators of the elements of τ_j. From a constructive point of view, initially we shall obtain τ_2 from the initial mesh τ_1, attending to the following fundamental considerations:
a) *8-subtetrahedron subdivision.* A tetrahedron $t_i^1 \in \tau_1$ is called of *type I* if $\epsilon_i^1 \geq \theta \epsilon_{\max}^1$. Later, this set of tetrahedra will be subdivided into 8 subtetrahedra as Figure 1(a) shows; 6 new nodes are introduced and its faces are subdivided as proposed by Bank [12].
Once the *type I* tetrahedral subdivision is defined, we can find neighbouring tetrahedra which may have 6, 5, ..., 1 or 0 new nodes introduced in their edges that must be taken into account in order to ensure the mesh conformity. We must remark that until the conformity of τ_2 is not ensured by marking edges, this new mesh will not be defined.
b) *Tetrahedra with 6, 5 or 4 new nodes.* Those tetrahedra are also considered as *type I*. Previously, the edges without new node must be marked.
c) *Tetrahedra with 3 new nodes.* In this case, we distinguish two situations:

c.1) If the 3 marked edges are not located on the same face, then we mark the others and the tetrahedron is introduced in the set of *type I* tetrahedra.
In the following cases, we shall not mark any edge, i.e., any new node will not be introduced in a tetrahedron for conformity. We shall subdivide them creating subtetrahedra which will be called *transient subtetrahedra.*

c.2) If the 3 marked edges are located on the same face of the tetrahedron, then 4 transient subtetrahedra are created as Figure 1(b) shows. The tetrahedra of τ_1 with these characteristics will be inserted in the set of *type II* tetrahedra.
d) *Tetrahedra with 2 new nodes.* Also here, we distinguish two situations:

d.1) If marked edges are not located on the same face, we construct 4 transient subtetrahedra. These tetrahedra are called *type III.a*; see Figure 1(c).

d.2) If the two marked edges are located on the same face, then 3 transient subtetrahedra are generated as Figure 1(d) shows. The longest marked edge is fixed as reference in order to take advantage in some cases of the properties of the bisection by the longest edge. These tetrahedra are called *type III.b.*
e) *Tetrahedra with 1 new node.* Two transient subtetrahedra will be created as we can see in Figure 1(e). This set of tetrahedra is called *type IV.*
f) *Tetrahedra without new node.* These tetrahedra of τ_1 are not divided and they will be inherit by the refined mesh τ_2. We call them *type V*; see Figure 1(f).

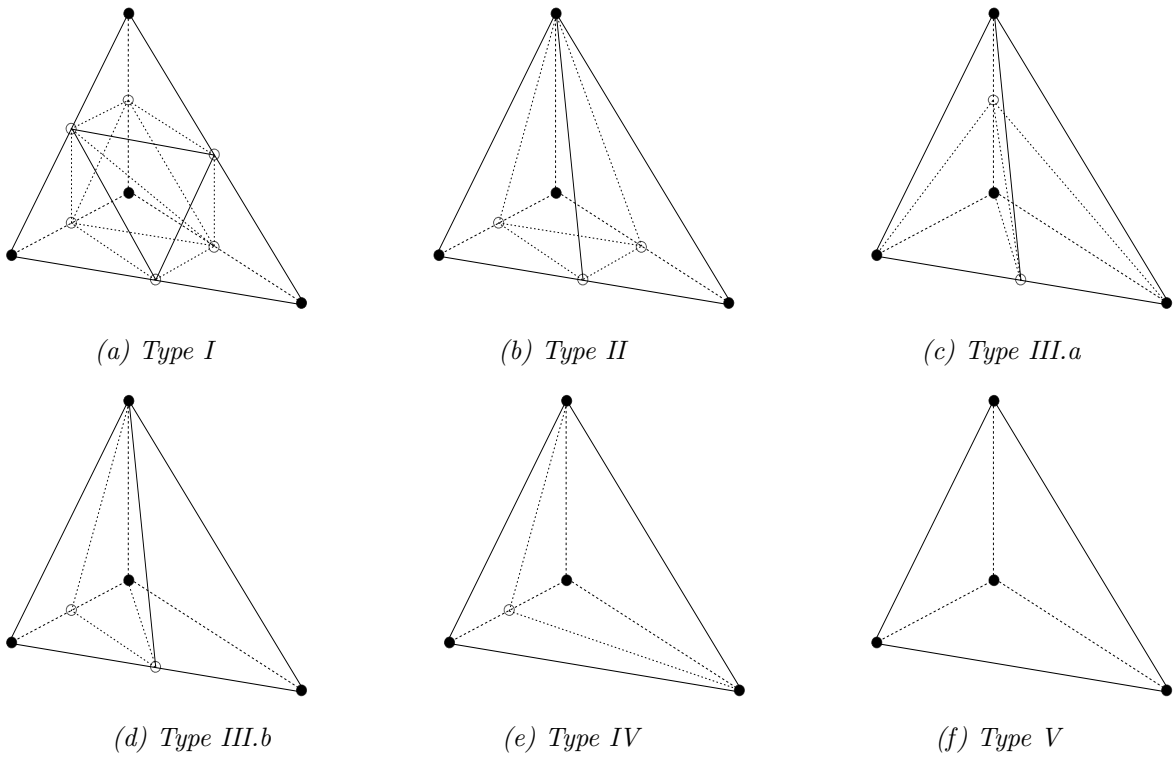

(a) Type I *(b) Type II* *(c) Type III.a*

(d) Type III.b *(e) Type IV* *(f) Type V*

Fig. 1 Subdivision classification related to the new nodes (empty circles)

VELOCITY FIELD MODELLING

We consider a mass consistent model for wind field adjustment which are based on the continuity equation and the impermeability conditions on the terrain Γ_b,

$$\vec{\nabla} \cdot \vec{u} = 0 \qquad \text{in } \Omega \tag{1}$$

$$\vec{n} \cdot \vec{u} = 0 \qquad \text{on } \Gamma_b \tag{2}$$

assuming that the air density is constant in the whole domain. We formulate a least-square problem in the domain Ω with the wind $\vec{u}(\widetilde{u},\widetilde{v},\widetilde{w})$ to be adjusted and the observed wind $\vec{v}_0(u_0,v_0,w_0)$. Lagrange multiplier technique is used to solve this problem, whose minimum comes to form the Euler-Lagrange equations and yields an elliptic equation and boundary conditions in the Lagrange multiplier ϕ

$$\frac{\partial^2\phi}{\partial x^2}+\frac{\partial^2\phi}{\partial y^2}+\frac{T_v}{T_h}\frac{\partial^2\phi}{\partial z^2}=-\frac{1}{T_h}\left(\frac{\partial u_0}{\partial x}+\frac{\partial v_0}{\partial y}+\frac{\partial w_0}{\partial z}\right) \quad \text{in } \Omega \tag{3}$$

$$\phi=0 \quad \text{on} \quad \Gamma_a \tag{4}$$

$$\vec{n}\cdot T\,\vec{\nabla}\phi=-\vec{n}\cdot\vec{v}_0 \quad \text{on} \quad \Gamma_b \tag{5}$$

We have used a discretization with tetrahedral finite elements for solving the above problem. To obtain the observed wind, horizontal interpolation of the station measures is carried out. Then, a log-linear wind profile is built up to the surface layer taking into account the horizontal interpolation, the effect of roughness on the wind velocity and air stability. Above the surface layer, a linear interpolation is carried out using the geostrophic wind. For more details see [13, 14].

1. Vertical velocity correction along the plume trajectory The main idea is to add to the interpolated wind field, which usually only consider the horizontal components of wind velocities, a vertical velocity along the trajectory of a pollutant plume arising from a chimney. Thus, the velocity field is origined by the wind and the vertical velocity of the pollutant. Gaussian plume models allow to approximate the effective height of a plume z_H and the horizontal distance d_f from the stack to the point where the plume height reaches z_H, depending on the emission characteristics, the wind and the atmospheric stability. Gases rise from the stack if their density is lower than the air density (buoyancy rise) or if they are at enough velocity which provides them a kinetic energy (momentum rise). In order to compute the effective height of the plume, we use Briggs' equations (see e.g. [15]). The height z_c of the chimney is replaced in practice by the height z_c', which is slightly lower than z_c when the emission velocity of gases w_c is less than 1.5 times the wind velocity (*Stack Downwash*),

$$z_c'=z_c \qquad \text{if } w_c\geq 1.5\left|\vec{v}_0\left(x_c,y_c,z_c\right)\right| \tag{6}$$

$$z_c'=z_c+2D_c\left[\left(w_c/\left|\vec{v}_0\left(x_c,y_c,z_c\right)\right|\right)-1.5\right] \qquad \text{if } w_c<1.5\left|\vec{v}_0\left(x_c,y_c,z_c\right)\right| \tag{7}$$

being (x_c,y_c,z_c) and D_c, the coordinates of the centre and the diameter of the emission surface, respectively. In addition, it can be distiguished the following cases:
a) If the buoyancy rise is predominant, i.e., $\dfrac{w_c}{\left|\vec{v}_0\left(x_c,y_c,z_c\right)\right|}\leq 4$, we define the buoyancy flow parameter as $F=gw_cD_c^2\dfrac{T_c-T}{4T_c}$, where g is the gravitational acceleration, T_c the temperature of stack gases in K and T the environmental temperature in K. For unstable or neutral atmospheric conditions, z_H and d_f may be approximated in m as,

$$z_H=z_c'+21.425\frac{F^{3/4}}{\left|\vec{v}_0\left(x_c,y_c,z_c\right)\right|} \qquad d_f=49F^{5/8} \qquad \text{if } F<55 \tag{8}$$

$$z_H=z_c'+38.71\frac{F^{3/5}}{\left|\vec{v}_0\left(x_c,y_c,z_c\right)\right|} \qquad d_f=119F^{2/5} \qquad \text{if } F\geq 55 \tag{9}$$

However, for stable conditions we define the stability parameter $s=\dfrac{g}{T}\dfrac{\Delta\theta}{\Delta z}$, where $\dfrac{\Delta\theta}{\Delta z}$ represents the variation of the potential temperature θ with height. If $\left|\vec{v}_0\left(x_c,y_c,z_c\right)\right|\geq 0.2746F^{1/4}s^{1/8}$, then we compute

$$z_H=z_c'+2.6\left(\frac{F}{s\left|\vec{v}_0\left(x_c,y_c,z_c\right)\right|}\right)^{1/3} \qquad d_f=2.07\left|\vec{v}_0\left(x_c,y_c,z_c\right)\right|s^{-1/2} \tag{10}$$

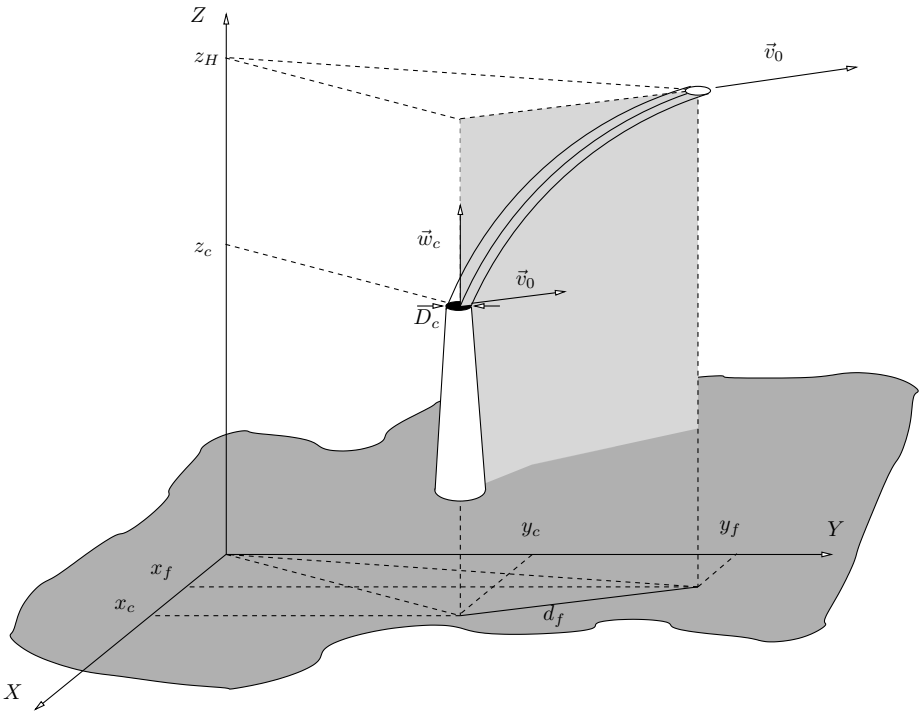

Fig. 2 Predominant buoyancy rise, except for stable conditions and calm wind

On the contrary, for low velocities of wind, i.e., $|\vec{v}_0\,(x_c, y_c, z_c)| < 0.2746F^{1/4}s^{1/8}$, it yields $d_f = 0$ and

$$z_H = z_c' + 4F^{1/4}s^{-3/8} \tag{11}$$

Using the computed values of z_H and d_f, except for stable conditions and calm wind, we propose to adjust the vertical component of the velocity along the trajectory of the plume by a linearly unaccelerated motion. In addition, the horizontal motion from the source to the distance d_f is considered uniformly accelerated. Thus, the time t_f corresponding to the distance d_f is,

$$t_f = \frac{1}{a_d}\left(-|\vec{v}_0(x_c, y_c, z_c)| + \sqrt{|\vec{v}_0(x_c, y_c, z_c)|^2 + 2a_d d_f}\right) \tag{12}$$

where $d_f = \sqrt{(x_f - x_c)^2 + (y_f - y_c)^2}$, with x_f, y_f being the horizontal coordinates of the point of maximum rise of the plume and a_d the horizontal acceleration with (a_{dx}, a_{dy}) in the same direction that $\vec{v}_0(x_c, y_c, z_c)$. The vertical acceleration a_0, the vertical velocity w_0 and the trajectory of the plume are then given by the following functions of the parameter t,

$$a_0(t) = \frac{-4w_c t_f + 6(z_H - z_c')}{t_f^2} + \frac{6w_c t_f - 12(z_H - z_c')}{t_f^3}t \tag{13}$$

$$w_0(t) = w_c + \frac{-4w_c t_f + 6(z_H - z_c')}{t_f^2}t + \frac{3w_c t_f - 6(z_H - z_c')}{t_f^3}t^2 \tag{14}$$

$$x(t) = x_c + u_0(x_c, y_c, z_c)t + \frac{1}{2}a_{dx}t^2 \tag{15}$$

$$y(t) = y_c + v_0(x_c, y_c, z_c)t + \frac{1}{2}a_{dy}t^2 \tag{16}$$

$$z(t) = z_c' + w_c t + \frac{-2w_c t_f + 3(z_H - z_c')}{t_f^2}t^2 + \frac{w_c t_f - 2(z_H - z_c')}{t_f^3}t^3 \tag{17}$$

If we suppose $a_0(t) \leq 0$ along the trajectory, we obtain between $t = 0$ and $t = t_f$,

$$\frac{3}{2}\left(z_H - z_c'\right) \leq w_c t_f \leq 3\left(z_H - z_c'\right) \tag{18}$$

This yields the following condition on a_d,

$$a_d = (1+\delta)\frac{2w_c}{3(z_H - z_c')}\left[(1+\delta)\frac{w_c}{3(z_H - z_c')}d_f - |\vec{v}_0(x_c, y_c, z_c)|\right] \tag{19}$$

being $0 \leq \delta \leq 1$. For $\delta = 0$, the value of t_f is related to the upper bound in (18) and, for $\delta = 1$, to the lower bound. The case $\delta = 1/2$ corresponds to a value of t_f which produces a constant vertical acceleration, a linear vertical component of velocity and a quadratic $z(t)$. If $w_c t_f - 2(z_H - z_c') \neq 0$, for a given value of z, the computation of the corresponding value of parameter t is carried out solving the cubic polynomial equation related to equation (17). The vertical component of velocity $\vec{v}_0$ is modified in any point of the domain Ω located inside a cylinder generated by the circular emission surface of the gases (of diameter D_c) which is moving parallel to the horizontal plane, along the parametric curve given by equations (15), (16) and (17) between $t = 0$ and $t = t_f$. For this purpose, we compute the distance from a given point (x_0, y_0, z_0) to the curve, $d_0^2 = (x(t_0) - x_0)^2 + (y(t_0) - y_0)^2$. If $d_0 \leq D_c/2$, then the vertical component of velocity in such point is fixed as $w_0(t_0)$, being t_0 the value of t relative to z_0 which is the solution of equation (17). Thus, constant vertical velocities are generated in the cylinder for each horizontal disk (see Fig. 2).

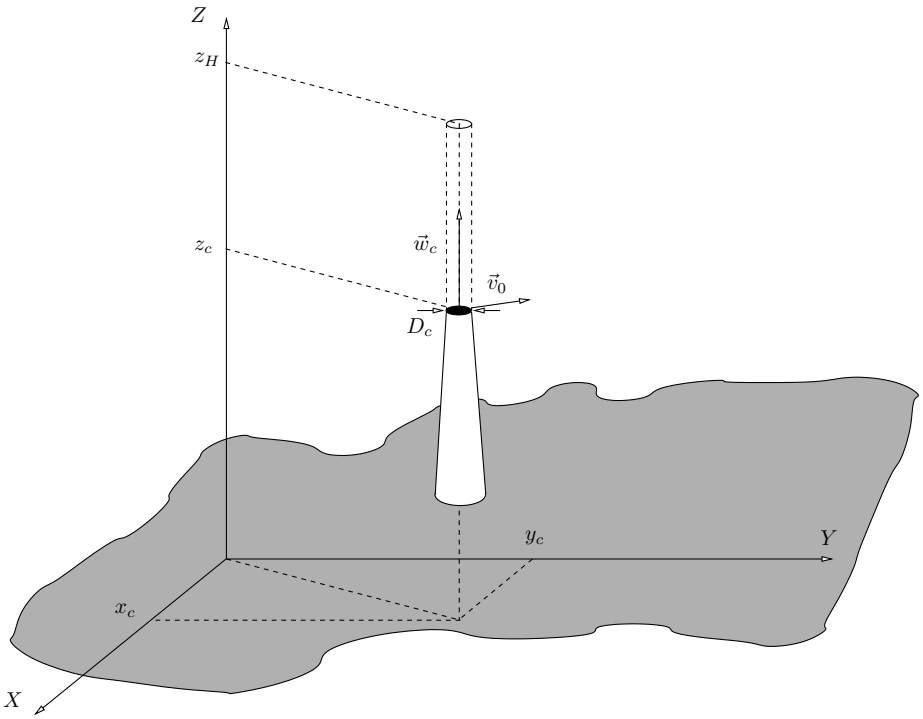

Fig. 3 Predominant momentum rise or buoyancy rise for stable conditions and calm wind

b) If $\dfrac{w_c}{|\vec{v}_0(x_c, y_c, z_c)|} > 4$, the predominant phenomenon is the momentum rise. In this case, $d_f = 0$ and $z_c' = z_c$. For unstable or neutral conditions we have,

$$z_H = z_c + \frac{3D_c w_c}{|\vec{v}_0(x_c, y_c, z_c)|} \tag{20}$$

On the contrary, for stable conditions z_H should be defined by the lower value of (20) and (21),

$$z_H = z_c + 1.5 \left[\frac{D_c^2 w_c^2 T}{4 T_c \left| \vec{v}_0 \left(x_c, y_c, z_c \right) \right|} \right]^{1/3} s^{-1/6} \tag{21}$$

In both situations, momentum rise or buoyancy rise with stable condition and calm wind, the horizontal motion of the plume until reaching the effective height is very small. Thus the trajectory of the gases is nearly vertical (see Fig. 3). In this case, we consider a uniformly unaccelerated motion. So, the value of parameter t related to the effective height of the plume z_H is $t_f = \dfrac{2\left(z_H - z_c\right)}{w_c}$ and the acceleration, $a_0 = \dfrac{-w_c}{t_f}$. Thus, the vertical velocity at a point of height z is $w_0(z) = w_c \sqrt{1 - \dfrac{2\left(z - z_c\right)}{w_c t_f}}$. Here, the vertical component of the velocity is modified inside a standard cylinder of which base is the emission surface of the gases in the stack and its height is $z_H - z_c$. So, we only attend to points (x_0, y_0, z_0), with $z_c \leq z_0 \leq z_H$, that verify the condition, $\sqrt{(x_c - x_0)^2 + (y_c - y_0)^2} \leq D_c/2$. We add a vertical velocity $w_0(z_0)$ at these points.

NUMERICAL EXPERIMENTS

For air pollution modelling of a test power plant located in the region of La Palma Island, we have to add the chimney geometry to the topographical data and apply the 3-D mesh generator. Let us consider a chimney with a height of 200 m over the terrain and diameter of 20 m at its top and 40 m at its bottom. Since, the mesh must be able to detect the details of the chimney, if we decide a size of elements about 2×2 m in the chimney, starting from the uniform 2-D mesh τ_1 of the rectangular area with a size of elements about 2×2 km, we should make ten global refinement steps using Rivara 4-T algorithm [16]. However, we only need five global refinement steps over τ_1 and, after, five local refinement of the elements inside the chimney.

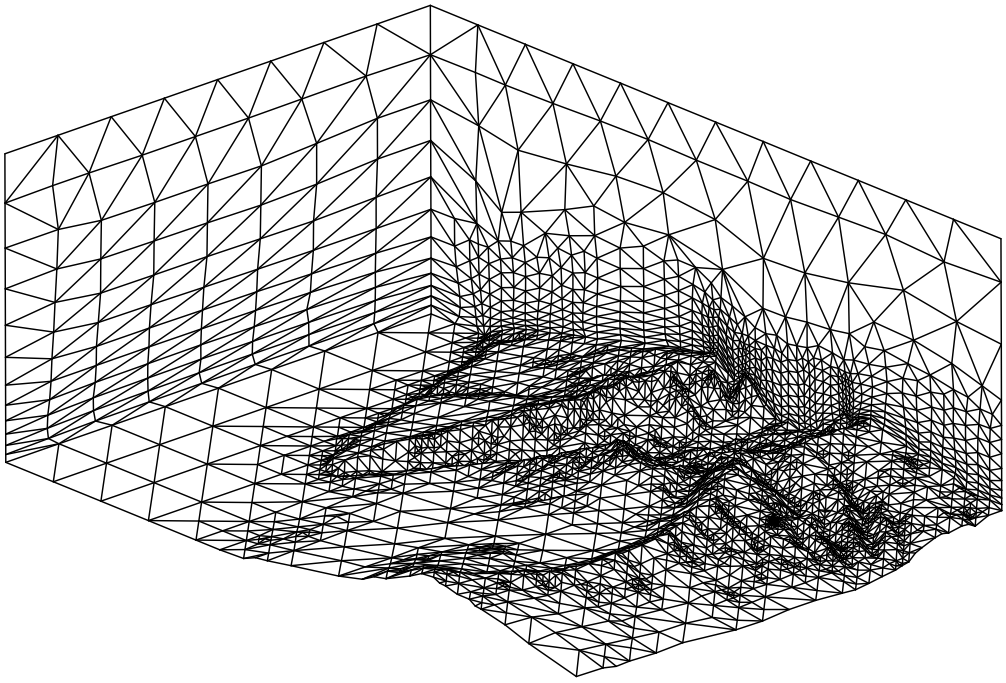

Fig. 4 Detail of 3-D adaptive mesh of La Palma Island

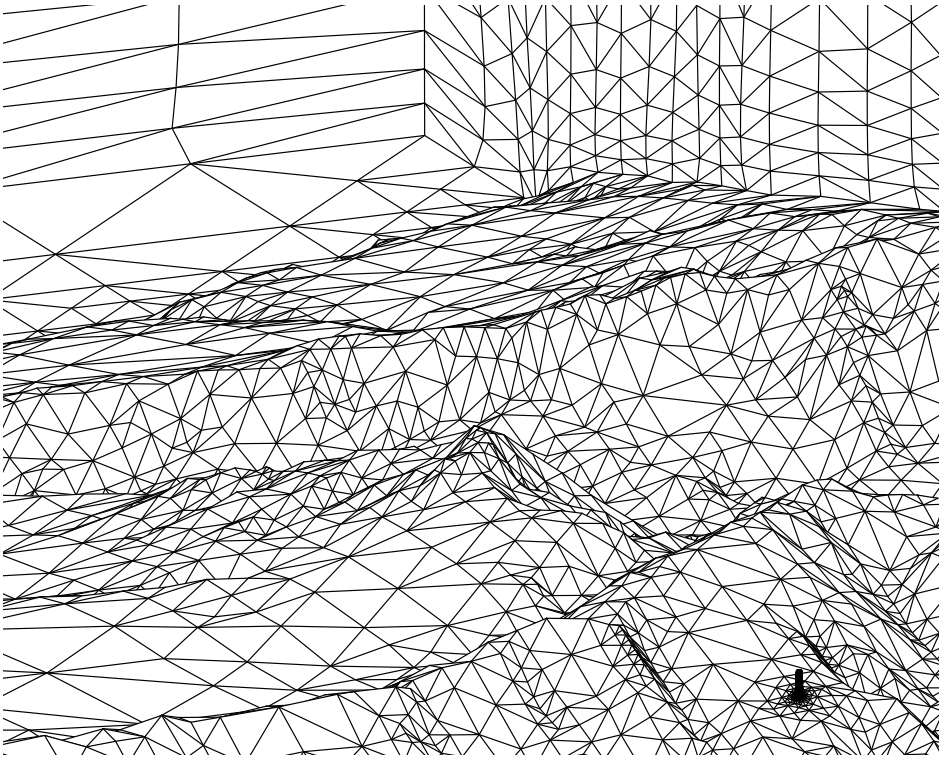

Fig. 5 Zoom in figure 4 including the chimney near the right bottom corner

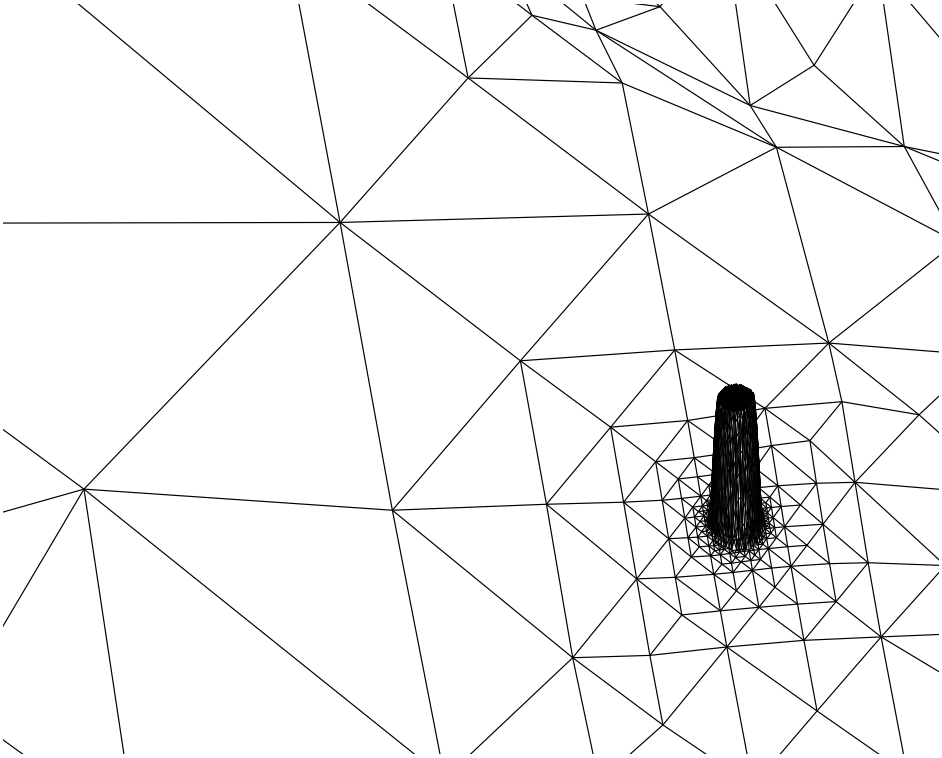

Fig. 6 Detail of the mesh in the sourroundings of the chimney

In this case, we applied the derefinement algorithm with a parameter $\varepsilon = 40\ m$ considering that nodes inside the chimney could not be eliminated. Finally, we have applied six local refinement steps in the plume trajectory to previous resulting 3-D mesh in order to obtain a new mesh with 31555 nodes and 170784 tetrahedra. Figures 4-6 show three details of the mesh in different scales. Figure 7 represents a detail of the adjusted velocity field $\vec{u}$ where the effect of chimney emission has been introduced.

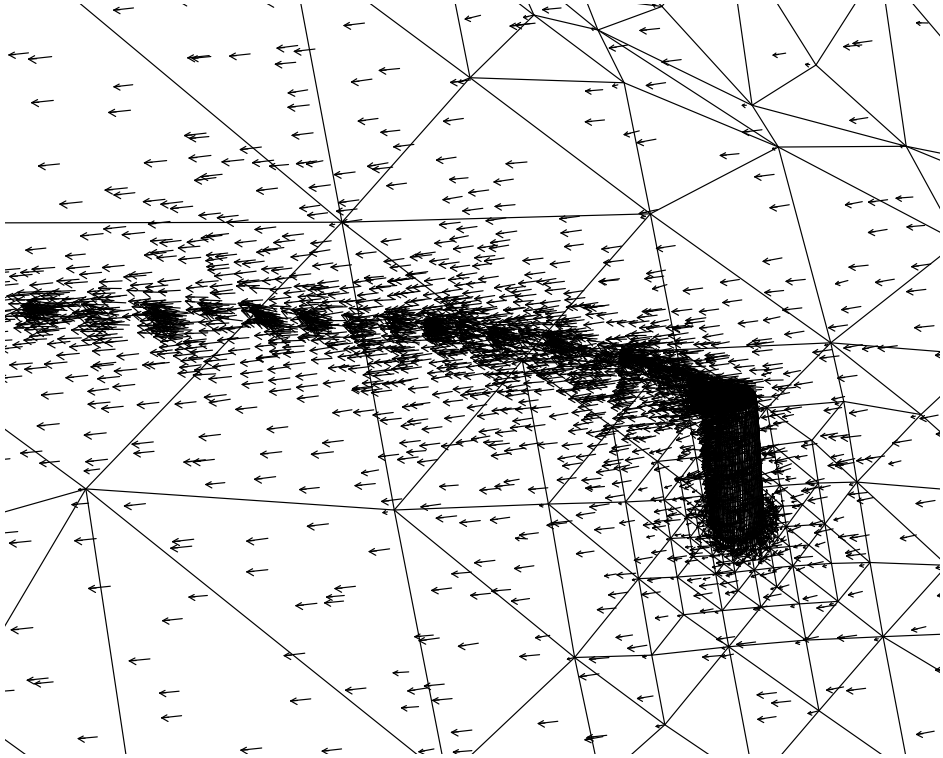

Fig. 7 Velocity field related to figure 6

CONCLUSIONS

We have presented an efficient technique for automatic and adaptive 3-D mesh generation in environmental problems. So, we can discretize domains defined over complex terrains which may include several chimneys, with a minimal user intervention and low computational cost. The local refinement of mesh in the pollutant plume allows to define a velocity field that takes into account the observed wind and the velocity of emission of gases from the chimney. This velocity field could be used for air pollution simulation.

Acknowledgements This work has been partially supported by the Spanish Government (Ministerio de Ciencia y Tecnología) and FEDER, grant number REN2001-0925-C03-02/CLI.

REFERENCES

[1] R. Montenegro, G. Montero, J.M. Escobar, E. Rodríguez, J.M. González-Yuste, *Tetrahedral mesh generation for environmental problems over complex terrains*, in P.M.A. Sloot, C.J.K. Tan, J.J. Dongarra, A.G. Hoekstra eds. *Computational Science-ICCS'2002. Lecture Notes in Computer Science, vol. 2329*, Springer-Verlag, Berlin Heidelberg New York (2002), pp. 335-344.

[2] R. Montenegro, G. Montero, J.M. Escobar, E. Rodríguez, *Efficient strategies for adaptive 3-D mesh generation over complex orography*, Neural, Parallel & Scientific Computation, 10(1), (2002), 57-76.

[3] P.L. George, F. Hecht, E. Saltel, *Automatic mesh generation with specified boundary*, Comp. Meth. Appl. Mech. Engng., 92, (1991), 269-288.

[4] L. Ferragut, R. Montenegro, A. Plaza, *Efficient refinement/derefinement algorithm of nested meshes to solve evolution problems*, Comm. Numer. Meth. Engng., 10, (1994), 403-412.

[5] A. Plaza, R. Montenegro, F. Ferragut, *An improved derefinement algorithm of nested meshes*, Adv. Engng. Soft., 27(1/2), (1996), 51-57.

[6] J.M. Escobar, R. Montenegro, *Several aspects of three-dimensional Delaunay triangulation*, Adv. Engng. Soft., 27(1/2), (1996), 27-39.

[7] J.M. Escobar, E. Rodríguez, R. Montenegro, G. Montero, J.M. González-Yuste, *Simultaneous untangling and smoothing of tetrahedral meshes*, Comp. Meth. Appl. Mech. Engng., 192, (2003), 2775-2787.

[8] M.S. Bazaraa, H.D. Sherali, C.M. Shetty, *Nonlinear Programming: Theory and Algorithms*, John Wiley and Sons, Inc., New York (1993).

[9] P.M. Knupp, *Algebraic mesh quality metrics*, SIAM J. Sci. Comput., 23, (2001), 193-218.

[10] J.M. González-Yuste, R. Montenegro, J.M. Escobar, G. Montero, E. Rodríguez, *An object oriented method for tetrahedral mesh refinement*, Adv. Engng. Soft., in press.

[11] R. Lohner, J.D. Baum, *Adaptive h-refinement on 3D unstructured grids for transient problems*, Int. J. Num. Meth. Fluids, 14, (1992), 1407-1419.

[12] R.E. Bank, A.H. Sherman, A. Weiser, *Refinement algorithms and data structures for regular local mesh refinement*, Scientific Computing IMACS, North-Holland, (1983), 3-17.

[13] G. Montero, R. Montenegro, J.M. Escobar, *A 3-D Model for wind field adjustment*, J. Wind Engng. & Ind. Aer., 74-76, (1998), 249-261.

[14] G. Montero, N. Sanín, *3-D modelling of wind field adjustment using finite differences in a terrain conformal coordinate system*, J. Wind Engng. & Ind. Aer., 89, (2001), 471-488.

[15] R.W. Boubel, D.L. Fox, D.B. Turner, A.C. Stern, *Fundamentals of Air Pollution*, Academic Press, San Diego (1994).

[16] M.C. Rivara, *A grid generator based on 4-triangles conforming. Mesh-refinement algorithms*, Int. J. Num. Meth. Engng., 24, (1987), 1343-1354.